ISSN 1063-455X, Journal of Water Chemistry and Technology, 2020, Vol. 42, No. 6, pp. 441–449. © Allerton Press, Inc., 2020.

PHYSICAL CHEMISTRY
OF WATER TREATMENT PROCESSES

Dye Adsorption on UiO-66: the Importance of Electrostatic Attraction Mechanism

Tran Ba Luan*

Department of Applied Science and Biology, Vinh Long University of Technology Education, Vinh Long City, Vietnam

**e-mail: luantb@vlute.edu.vn*

Received January 19, 2019; revised November 21, 2019; accepted March 3, 2020

Abstract—Adsorption is known as the best technique to remove dyes from waste water, and the choice of adsorbent is the most important factor. In this regard, some commercial porous materials have been applied for a long time as popular adsorbents for dye adsorption. However, the search for new classes of porous materials is still attractive to researchers. Recently, metal-organic frameworks are seen to be promising candidates as adsorbents for dyes due to their large surface area, ordering, and flexible structure. There are some possible mechanisms for the dye adsorption in water performed on metal-organic frameworks, including the electrostatic interaction forming attractive charge of dye molecules and adsorbents, π–π stacking of organic rings from dye and metal-organic frameworks, hydrogen bonding between the dye and hydroxyl group of the metal-organic frameworks, hydrophobic interaction, acid-base interaction and effect of framework structure. Among them, the electrostatic attraction mechanism plays an important role in dye adsorption on MOFs, highlighting differences as compared to traditional adsorbents in this field. This work is the first detailed investigation into the effect of electrostatic attraction mechanism in dye adsorption on UiO-66 and their modifications. Two samples of Co/UiO-66 and H^+/UiO-66 were prepared under normal stirring and heating conditions to increase the positive charge of the surface. The characterization using powder X-ray diffraction (XRD), scanning electron microscopy (SEM) and FTIR indicated the existence of proton on UiO-66, while Raman spectroscopy and inductively coupled plasma mass spectrometry (ICP-MS) confirmed the successful addition of cobalt into the UiO-66 structure at the amount of about 0.6 wt %. Results obtained for methyl orange (MO) adsorption on the surface have shown enhanced adsorption capacity for both Co-UiO-66 and H^+/UiO-66 as compared to parent UiO-66. Moreover, the experiments with highly selective removal of anionic dye as compared to cationic dye were performed and explained in detail for mixed dye solutions of MO with methylene blue (MB), indicating the important role of electrostatic attraction mechanism. Notably, it is shown that the addition of Co to UiO-66 results in a higher effect of electrostatic interaction than that of H^+.

Keywords: electrostatic attraction, Co doped on UiO-66, methyl orange dye, selectivity adsorption

DOI: 10.3103/S1063455X20060107

INTRODUCTION

Among metal-organic framework (MOF) materials, UiO-66 (Universitetet i Oslo) was shown to possess the perfect structure by the studies performed around ten years ago [1]. This material has quickly attracted the attention of researchers for many applications such as gas adsorption and separation, drug delivery, catalysis and sensing [2, 3]. As compared to other MOFs, UiO-66 exhibits multilateral covalence of Zr where 12 bridgings of –COOH are connected to $Zr_6O_4(OH)_4$ core to form rigid and stable secondary building (SBU) [1]. This explains that UiO-66 exhibits the most resistance towards water and some other solvents [4] capable to dissolve organic dyes. Moreover, such multiple coordination environments of ligands to inorganic nodes in UiO-66 can be easily modified to obtain materials usable as dye adsorbents [5, 6].

In fact, UiO-66 was proved to be promising for dye adsorption by some reports a few years ago. Chen [7] was the first publication where the successful preparation of UiO-66 and its functional amine group were reported, and good removal of anionic (methyl orange-MO, acid chrome blue K), cationic (methylene blue-MB) and neutral (Rhodamine B-RB, neutral red) dye was shown. The results demonstrated high selectivity removal of MO: 90% by (UiO-66) and 97.97% by (NH_2-UiO-66) at initial concentration of 20 mg/L. Besides, some modifications based on UiO-66 application for selective dye removal have also

been published, showing the important role of electrostatic attraction mechanism. Acid-promoted synthesis of UiO-66 for anionic dye removal was recorded by Zhang [8]. In this study, the UiO-66 was modulated by addition of HCl or CH_3COOH to create acid-promoted material with H^+ sites, which exhibits enhanced excellent selectivity for anionic MO, 6.4 times higher than that for MB due to the domination of electrostatic attraction forces. On the other hand, immobilized-phosphate composite (UiO-66-P) also fabricated in facile route, showed the efficient charge-selective capture of MB with high adsorption at 91.1 mg/g. Notably, the UiO-66-P exhibited an extremely improvement at 272% compared to that of initial UiO-66 for taking up cationic dye Methylene Blue (MB) [6].

Recently, Han [9] has successfully doped Ti^{4+}/UiO-66 to obtain material with promoted Congo red dye (CR) adsorption: 3 times higher than its parent Zr-UiO-66, as high as 979 mg/g. The increased dye adsorption capacity is attributed to electrostatic attraction mechanism. This was explained by increasing zeta potential point after doping UiO-66 by Ti^{4+}. Similarly, Ce(III) doped to UiO-66 was reported by Yang et al. [10]. The ratio Ce(III)/Zr(IV) in the sample attained to 39.1% while the pure phase of UiO-66 remained after the doping. The hybrid material exhibited higher adsorption capacity for some dyes: MB, MO, and CR due to an increase of $\pi-\pi$ attraction interaction, related to increased pore size and number of adsorption sites. Especially, the removal of cationic dye MB increased by a factor of 5.9 as compared to that of anionic dyes, dominated by the stronger electrostatic interaction because of decreased positive charge after doping by Ce(III).

Very recently, Li [11] reported a strategy for synthesis of MOFs which indicated the key role of electrostatic attraction mechanism in studying dye adsorption on this material. In this work, the multivariate UiO-66 was prepared with different ratios of Terephthalic acid (BDC)/Benzene-1,3,5-tricarboxylic acid (BTC) as ligands. The samples with addition of higher amount of BTC showed higher negative charge on the surface and smaller surface area due to deprotonating of uncoordinated carboxylic groups from BTC. Therefore, these samples showed enhanced adsorption selectivity of cationic dye (MB) as compared to anionic dye (MO) and neutral dye (RB) by 93.5 and 17.1%, respectively. This study presents strongly evidence which confirms high importance of electrostatic attraction mechanism for dye adsorption on MOFs.

These studies proved that the modification on UiO-66 is a promising topic for dye adsorption application, especially for the selective dye removal. Therefore, in our research the Co-UiO-66 and H^+/UiO-66 samples were synthesized in the facile procedure to enhance the positive charge on the surface, and then used as adsorbents. The characterization of the materials was performed using different techniques to confirm the occurrence of Co^{2+} and H^+ in the typical structure of UiO-66. These samples were applied for the removal of typical dyes, including anionic (methyl orange—MO) and cationic (methylene blue—MB) dyes to examine the efficiency and selectivity of anionic dye adsorption. The research aims to the detailed consideration of the influence of electrostatic attraction mechanism on adsorption, which is the most important application of MOFs in this field.

EXPERIMENTAL

Zirconium(IV) chloride ($ZrCl_4$, purity 98%, Acros), terephthalic acid (H_2BDC, purity 99%, Acros), cobalt(II) nitrate hexahydrate ($Co(NO_3)_2 \cdot 6H_2O$, purity 98%, Showa), acetic acid (99.7%, Aencore), and N,N-dimethylformamide (DMF, high purity solvent 98%, Tenda-USA) were used as precursors. The studied dyes were methyl orange (MO) and methylene blue (MB) as dye powder of purity 98% (Sigma-Aldrich). In a typical preparation, 0.3381 g of $ZrCl_4$ (1.5 mmol) and 0.25 g H_2BDC (1.5 mmol) were added to 40 mL of DMF. The mix was stirred at room temperature for 60 min. The mixture was then sealed in a 50 mL Teflon autoclave and heated to 140°C for 8 h. The powders were collected by filtration, then washed 3 times with DMF and 3 times by methanol, dried at 60°C overnight to form UiO-66 hereinafter referred to as U-0. In the similar process, 1.7 mL CH_3COOH also was added to the solution before stirring and heated as explained above; the resulting material is referred to below as UA-0.

The incorporation of Co on UiO-66 was carried out for both sample above, adding $Co(NO_3)_2$ (0.225 mmol) to initial solution to produce slightly blue powder named U-1, UA-1, thus modifying U-0 and UA-0, respectively.

Characterizations

X-ray powder diffraction (XRD) patterns were recorded using a CuK_α radiation (40 mA and 40 kV) source on a D8 Advance Bruker powder diffractometer at a scan rate of 3°/min with a step size of 0.03°.

Scanning electron microscopy (SEM) studies were performed on a JEOL JSM-7600F operated at 15 kV. Raman Spectroscopy (Andor Solis) was used to record the spectra of powder at room temperature within a wavelength range of 500–1800 cm^{-1}. Inductively coupled plasma mass spectrometry (ICP-MS) Agilent 7500ce was used to detect metal concentration of Co and Zr. Nitrogen isotherm measurements were performed using a Micromeritics ASAP 2010. Samples were pre-treated by heating under vacuum at 120°C for 4 h. Zeta potential point was recorded by Dynamic Light Scattering (DLS) zeta-sizer of Nano-2S90 (Malvern). The activated power was dispersed in buffer solution pH7 and sonicated before testing.

Dye Removal Study

Typically, 10 mg of UiO-66 or related materials were added to 20 mL of MO dye aqueous in various concentration (50–250 mg/L) in a vial with cap; then the mixing was treated in an ultrasonic bath for 1 min to mix completely. For the selectivity dye adsorption, mixing of MO (25 mg/L) with MB (25 mg/L) was obtained similarly to above. The vial was stirred at room temperature at a different time from 5 to 120 min, then the solution was collected by a syringe filter (mesh of 0.22 μm). A UV-vis spectrometer (SCINCO S-3100) was used to record the absorbance change of the dye solution.

The recycling was carried out 4 times using methanol 95% only for eluting. After the MO adsorption process, the absorbent was collected and washed 3 times by eluting solution through centrifugation, then dried at 90°C overnight to use for the next time.

Adsorbed amount of dye q_t was calculated from the equation:

$$q_i = \frac{(C_0 - C_t)V}{m},$$

where C_0 is the initial concentration of dye solution (mg/L), C_t is the concentration of dye solution at time t (mg/L), V is the volume of dye solution (L), and m is the adsorbent mass (g).

RESULTS AND DISCUSSION

XRD Patterns

X-ray diffraction is the important data to identify the pure phase and structure of materials. As seen in Fig. 1a, the powder XRD patterns of U-1 and UA-1 almost matched their parent UiO-66 pattern and agree well with the literature data [1, 12] with two typical peaks located at $2\theta \sim 7°$ and 8°. The data indicated that the preparation of UIO-66 and their derivatives of doped Co^{2+} ions was achieved in pure phase, because no straight peaks were observed for both U-1 and UA-1 patterns. The 2θ shift forward towards a higher angle of 0.03° (U-1) and 0.12° (UA-1) after adding Co^{2+} ion was observed showing small change of the lattice in the frameworks. This change is the evidence that this metal occurs in the material, similarly to several reports on other systems of metal doped to MOFs, such as Zn doped on Ni-MOF [13], Co doped to MOF-5 [14] and Ti or Ce doped to UiO-66 [9, 15].

It is also apparent that Co ion signal at typical position 2θ of 20 and 32° is absent [16], indicating possibly that the metal is doped inside the UiO-66 framework. Also, the lower shift of 2θ from UA-0 and UA-1 as compared to U-0 and U-1 may be related to the presence of H^+ in the material, as was similarly observed by Qiu [9].

SEM and ICP-MS Results

SEM images showed the high crystallinity of all samples, which agrees with the sharp peaks in XRD patterns. The morphology of U-0 (Fig. 1b) shows small particle size (about 50 nm), which slightly increases when adding Co^{2+} ion to the synthesis process. However, the cube-like structure of UiO-66 becomes more uniform as is seen in Fig. 1c, similarly to the data reported previously by Mohammadi [17].

For sample obtained with addition of CH_3COOH, the aggregated structures were found to be octahedral for both UA-0 and UA-1 as seen in Fig. 1b (*3*, *4*); this is related to the absence of amorphous structures found in XRD patterns. In addition, FTIR spectra (Fig. 2b) show a stronger peak at the band around of 1252 cm^{-1} (indicating C–O stretching of terephtalic acid and a shift up at the band of 1580 cm^{-1} (related to O–C–O asymmetric stretching of carboxylic groups) [18] of UA-0 and UA-1, as compared to U-0 and U-1, respectively. This observation provided stronger evidence for grafting H^+ on the surface of UiO-66.

ICP-MS results indicated the existence of Coin materials with small concentration of 313.4 and 630.5 ppm for U-1 and UA-1, respectively. The higher concentration of Co for the sample with added ace-

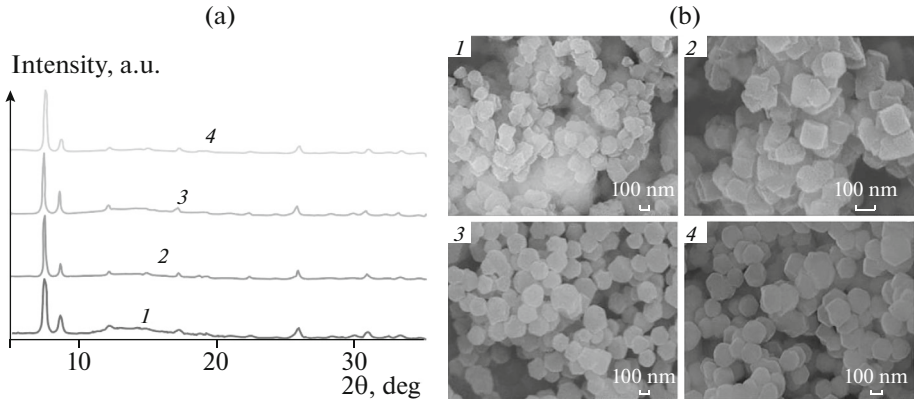

Fig. 1. XRD patterns of UiO-66 and Co/UiO-66 (a) and photo—SEM images (b) of: (*1*) U-0; (*2*) U-1; (*3*) UA-0; (*4*) UA-1.

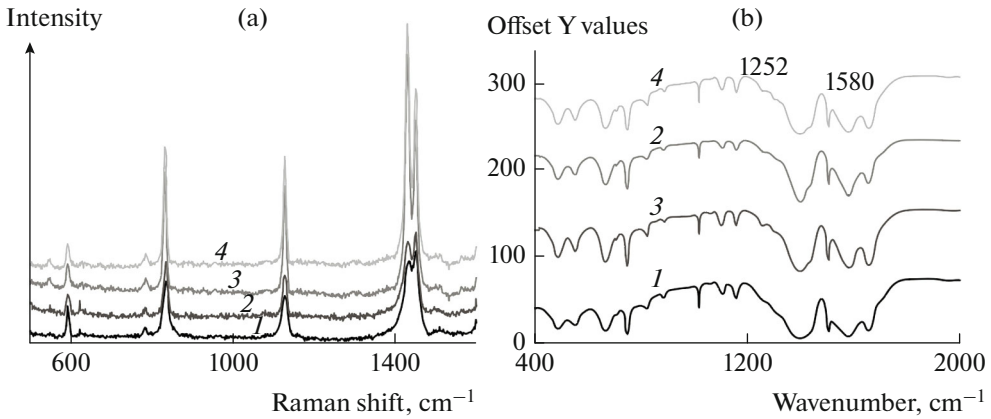

Fig. 2. (a) Raman spectra and (b) FTIR spectra of synthesized samples. (*1*) U-0; (*2*) U-1; (*3*) UA-0 and (*4*) UA-1, respectively.

tic acid can be explained by coordination of CH_3COOH to Zr cluster formation in nucleation process [8], which could result in easier incorporating of Co ions into Zr–O clusters. This matches with higher shift of the first peaks for UA-1 than for U-1, as observed in XRD patterns.

In other experiments, the synthesis described above was performed with higher ratio of Co/Zr (0.6 and 1.0) in an attempt to obtain higher Co doping to the framework. For the sample with ratio Co/Zr = 0.6, the concentration of Co doped to UiO-66 (ICP result of 704.5 ppm) was not much higher than that for ratio Co/Zr = 0.15. In addition, when the ratio Co/Zr was increased to 1 in the precursor, phase and morphology of this product had changed to low crystallization and more amorphous mix, as shown by weak intensity at typical peaks (7° and 8°) from XRD pattern and lack of crystals observed by SEM. These results mean that the ratio Co/Zr in synthesized precursor higher 0.15 is an overdose with regard to the attempts to increase the doping amount of Co to the UiO-66 framework by this procedure.

Raman Test

The Raman spectra in Fig. 2a are in agreement agrees with Atzori and Kandiah [18, 19] where key bands around of 1600 and 1420–1450 cm^{-1} were ascribed to symmetric stretching belonging to benzene ring (C=C) and organic benzene ring stretching (O–C–O), respectively [20]. For sample doped by Co (U-1 and UA-1), very small signal peaks rise at the band around 550 cm^{-1}, indicating the stretching of Co–O as mentioned in the literature [21, 22]. Also, lower shift of peaks was observed for U-1 and UA-1 as compared to U-0 and UA-0 at region 830 and 1420 cm^{-1} observed in small scale (evidencing the symmetric stretching of O–C–O bonding of ligands to inorganic clusters [18, 20, 23]), indicating that this

Table 1. pH level before and after adsorption

Time of adsorption, min	U-0	U-1	UA-0	UA-1
0	4.73	4.68	4.44	4.60
30	4.70	4.69	4.40	4.75
60	4.62	4.63	4.38	4.78
90	4.60	4.62	4.35	4.87
120	4.60	4.62	4.35	4.87

bonding is weaker due to increase of excited wavelength [24]. This change may be caused by doping of Co ions into the Zr–O clusters, creating new linking between Co and ligands, thus making the bonding force between ligands and hybrid Zr–O clusters weaker.

Effect of Electrostatic Attraction on Dye Removal

Four samples (U-0, U-1, UA-1, and UA-1) were tested for MO removal as typical examination of effects caused by doping Co on dye adsorption. The adsorption at conditions: 10 mg adsorbent, 20 mL MO of 50 mg/L at room temperature, attains the equilibrium state after 2 h, whereas the concentration of dye solution and pH level almost unchanged by time, as shown in Table 1, similar to the data reported in the literature [8] (see details in Table 1 and notes on adsorption kinetics below). As shown in Fig. 3a, the MO adsorption capacities attain the values 33, 75, 55 and 82 mg/g for U-0, U-1, UA-0, and UA-1, respectively. The changing of orange colour which becomes slightly lighter was observed clearly for U-1 and UA-1 after adsorption. On the other hand, the samples with added CH_3COOH show higher adsorption capacity than those without this addition by 20 mg/g for UA-0/U-0 and 10 mg/g for UA-1/U-1, due to the contribution of H^+ which exist on the surface of sorbent thus promoting electrostatic interaction [8]. However, the adsorption amount from Co doped samples as compared to their parents shows a higher increase as compared to added acid samples, reaches to 42 mg/g (U-1/U-0) and 27 mg/g (UA-1/UA-0). In addition, the zeta potential of a sample in aqueous solution increases in order UA-1 > U-1 > UA-0 > U-0, which demonstrates the corresponding increase of positive charge of the surface for these samples. Therefore, the MO adsorption capacity of four samples is also proportional to the increase of zeta potential. This indicates that the electrostatic attraction between the adsorbents and the MO caused by adding of Co ion on UiO-66 is higher that of H^+.

Herein, we assume that the Co ions incorporated weakly to Zr–O clusters (as shown by the characterization test above), became activated sites and promoted the anionic dye adsorption. It is also known that MO, because of its larger size, cannot enter inside small pore with size about 0.6 nm [1] of microporous UiO-66, and possibly adsorbs on the external or outer surface as reported in [7, 8]. Therefore, MO adsorption is promoted by the electrostatic interaction between positive charge of the sorbent and negatively

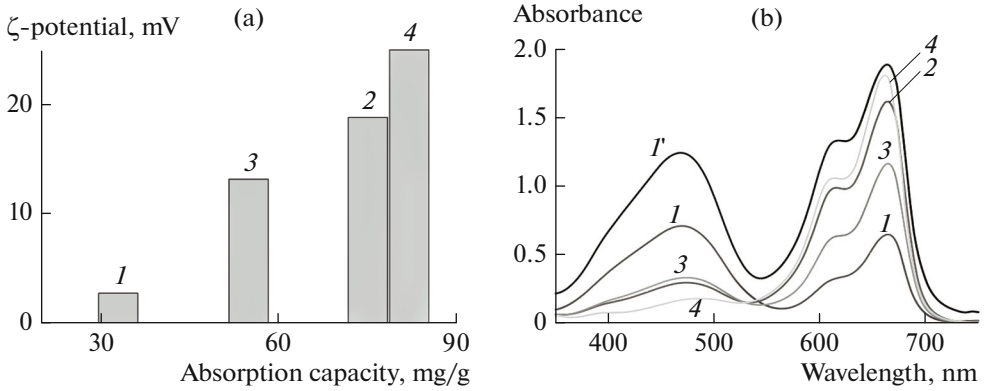

Fig. 3. (a) Zeta potential as versus of MO adsorption on samples and (b) related absorbance changing. (*1'*) Before; (*1*) U-0; (*2*) U-1; (*3*) UA-0; (*4*) UA-1. Condition adsorption: 10 mg adsorbent/20 mL of MO solution of 50 mg/L.

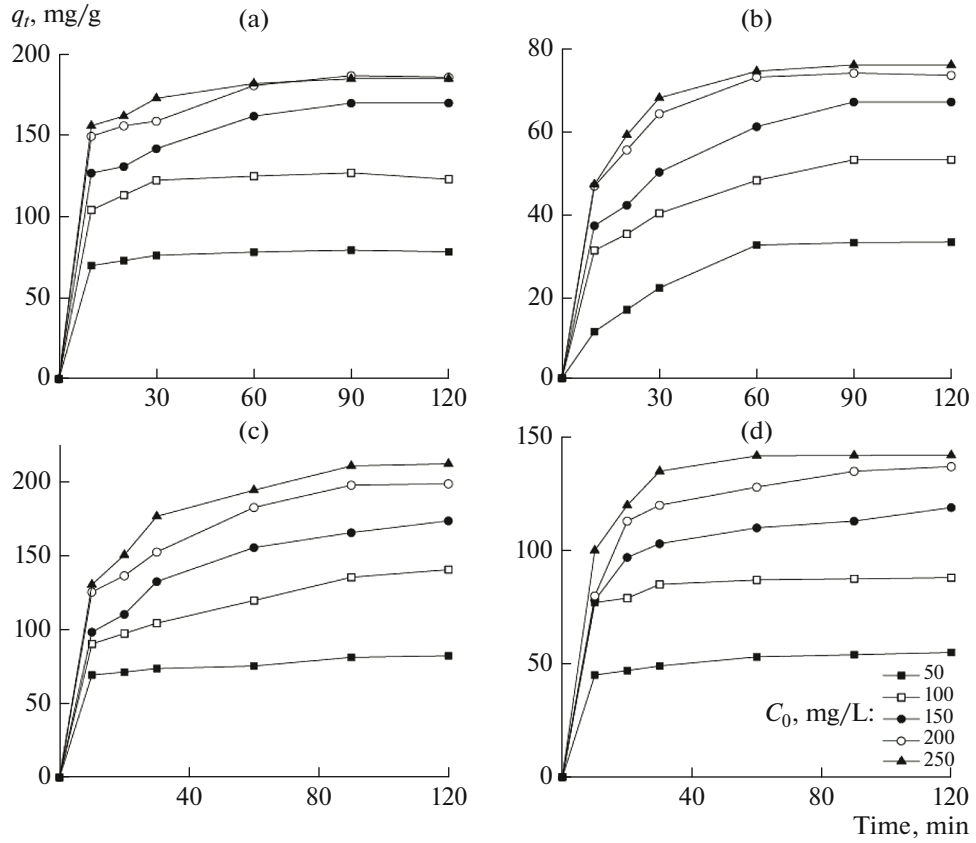

Fig. 4. Kinetic of adsorption on U-1 (a), U-0 (b), UA-1 (c) and UA-0 (d).

charged group (SO_3^-) and –N=N– in MO molecular structure [25], similarly to what was reported by Zhang [26].

Adsorption Kinetics

Figure 4 illustrates the dependence of adsorption on contact time for different MO concentrations (50, 100, 150, 200, and 250 mg/L) observed for four samples. The adsorption increases with the increase of MO initial concentration, approaches the values somewhat lower than the equilibrium value after 60 min of stirring, and then slowly increases to equilibrium value within 2 h, showing that the studied material is a good absorbent for dye treatment [7]. At higher concentration of 200 and 250 mg/L, the adsorption capacity attained 76.0, 185.0, 142.0 and 211 mg/g at equilibrium state for U-0, U-1, UA-0 and UA-1, respectively. Moreover, a slight increase in adsorption amount between concentration of 200 and 250 mg/L indicated that a saturation adsorption has been gained, as described by Liu [27]. In total, UA-1 and U-1 exhibit higher MO removal as compared to U-0 and UA-0 and the results reported in previous publication related to UiO-66 in [7, 8].

The Anionic Selectivity of Adsorption

The selective adsorption of anionic dye as compared to cationic dye (MB) is the most important section of the research aimed to prove the effectiveness of doping Co on UiO-66. The mixed dye solution of MO and MB was also tested for 2 h at a low concentration of 25 mg/L of each dye to verify the adsorption selectivity with respect to the anionic dye. The selectivity of MO/MB increases in order U-0 < UA-0 < U-1 < UA-1, along with the MO/MB removal selectivity of 42.4/65.6, 76.0/14.2,73.1/38.4 and 86.5/4.2% for U-0, U-1, UA-0 and UA-1, respectively (details in Fig. 3b). It should be noted that no MO concentration in the solution was observed after 120 min of adsorption, which follows from very small absorbance at a wavelength at 464 nm found in UA-1 spectra. As recorded, the colour changed from green or black

Table 2. Adsorption isotherm data

Sample	Langmuir			Freundlich		
	q_m, mg/g	K_L	R^2	K_f	n	R^2
U-0	103	0.01	0.9976	8.0	0.43	0.9874
U-1	212	0.04	0.9981	39.0	0.31	0.9720
UA-0	194	0.02	0.9945	15.3	0.44	0.9839
UA-1	232	0.05	0.9952	45.7	0.31	0.9917

(mix of MO/MB) to blue (MB) for UA-1 after adsorption. For U-1, the initial colour changes to light green after adsorption, showing a higher concentration of MB than MO in maintaining solution.

Adsorption Isotherm is used to characterise the process of adsorption on materials and estimate the highest adsorption capacity. In this study, the Langmuir and Freundlich isotherms are chosen as typical models in dye adsorption [28, 29], expressed by Eqs. (1) and (2), respectively:

$$q_e = \frac{q_m K_L C_e}{1 + K_L C_e}, \quad (1)$$

$$q_e = K_f C_e^{1/n}, \quad (2)$$

where q_e and q_m are MO adsorbed amounts at equilibrium and maximum sorption capacity adsorbents (mg/g), respectively, C_e is MO concentration at equilibrium state and K_L, K_f and n are Langmuir and Freundlich isotherm constants, respectively. It is seen from Table 2, that the Langmuir isotherm provides for a better fit and is more applicable than Freundlich model, as follows from the fact that the correlation coefficient calculated from Langmuir model ($R^2 > 0.99$) is higher than that calculated from Freundlich model. Also, the coefficient of Freundlich model $n < 1$ indicates poor adsorption characteristic to this model [30]. This fitting to model isotherm shows that the adsorption process is mainly monolayer on the surface of the sorbent and the maximum MO adsorption capacity attains 103, 212, 194 and 232 mg/g for U-0, U-1, UA-0 and UA-1, respectively. The simulated adsorption capacity by Langmuir is close to experiment data, implying that the adsorption reached its equilibrium value.

In our study, U-1 and UA-1 show higher ratio MO/MB removal than that reported by Zhang using high concentration CH_3COOH in the synthesis UiO-66 [8]. Obviously, the active metal Co doped under simple route is a crucial factor in high enhance and selectivity of the removal of anionic dye as compared to cationic dye. This selectivity may be related to the increased positive charge on the surface of the material due to the doping of Co^{2+}, similar to what was observed by Han [9]. Also, the addition of Co to UiO-66 resulted in higher electrostatic attraction for anionic MO and repulsion for cationic MB as compared to that of H+ or initial sample.

CONCLUSIONS

In this research, the simple doping of Co to Zr-UiO-66 was performed at a small concentration of Co (0.6 wt %) in the framework, but in the amount high enough to make the hybrid MOFs perfect. Also, a facial synthesis of H^+/UiO-66 was performed in the same way as described above. The materials were characterized by typical physical methods including XRD, Raman spectra, SEM and ICP-MS to confirm the occurrence of these active agents. The results confirm the existence of H^+ and Co on UiO-66 at a small amount.

The adsorption capacity attained higher value as compared to the previous report in this field. The high selectivity adsorption of MO compared to that of MB obtained on Co-doped UiO-66 samples (U-1 and UA-1) are the most interesting results of the study, indicating the domination of electrostatic attraction mechanism in the dye adsorption process. It should be stressed that the effect of adding Cobalt (Co^{2+}) to electrostatic attraction between the adsorbent and dye is higher than that of H^+.

REFERENCES

1. Cavka, J.H., Jakobsen S., Olsbye U., Guillou N., Lamberti C., Bordiga S., and Lillerud, K.P., A new zirconium inorganic building brick forming metal organic frameworks with exceptional stability, *J. Am. Chem. Soc.*, 2008, vol. 130, no. 42, pp. 13850–13851.

2. Aceituno Melgar, V.M., Kim, J., and Othman, M.R., Zeolitic imidazolate framework membranes for gas separation: A review of synthesis methods and gas separation performance, *J. Ind. Eng. Chem.*, 2015, vol. 28, pp. 1–15.
3. Zhang, K., Lively, R.P., Dose, M.E., Brown, A.J., Zhang, C., Chung, J., Nair, S., Koros, W.J., and Chance, R.R., Alcohol and water adsorption in zeolitic imidazolate frameworks, *Chem. Commun.* (Cambridge), 2013, vol. 49, no. 31, pp. 7–3245.
4. Schaate, A., Roy, P., Godt, A., Lippke, J., Waltz, F., Wiebcke, M., and Behrens, P., Modulated synthesis of Zr-based metal-organic frameworks: From nano to single crystals, *Chem.–Eur. J.*, 2011, vol. 17, no. 24, pp. 6643–6651.
5. Wang, K., Li, C., Liang, Y., Han, T., Huang, H., Yang, Q., Liu, D., and Zhong, C., Rational construction of defects in a metal-organic framework for highly efficient adsorption and separation of dyes, *Chem. Eng. J.*, 2016, vol. 289, pp. 486–493.
6. Yang, J.-M., A facile approach to fabricate an immobilized-phosphate zirconium-based metal-organic framework composite (UiO-66-P) and its activity in the adsorption and separation of organic dyes, *J. Colloid Interface Sci.*, 2017, vol. 505, pp. 178–185.
7. Chen, Q., He, Q., Lv, M., Xu, Y., Yang, H., Liu, X., and Wei, F., Selective adsorption of cationic dyes by UiO-66-NH_2, *Appl. Surf. Sci.*, 2015, vol. 327, pp. 77–85.
8. Qiu, J., Feng, Y., Zhang, X., Jia, M., and Yao, J., Acid-promoted synthesis of UiO-66 for highly selective adsorption of anionic dyes: Adsorption performance and mechanisms, *J. Colloid Interface Sci.*, 2017, vol. 499, pp. 151–158.
9. Han, Y., Liu, M., Li, K., Sun, Q., Zhang, W., Song, C., Zhang, G., Conrad Zhang, Z., and Guo, X., In situ synthesis of titanium doped hybrid metal-organic framework UiO-66 with enhanced adsorption capacity for organic dyes, *Inorg. Chem. Front.*, 2017, vol. 4, no. 11, pp. 1870–1880.
10. Yang, J.-M., Ying, R.-J., Han, C.-X., Hu, Q.-T., Xu, H.-M., Li, J.-H., Wang, Q., and Zhang, W., Adsorptive removal of organic dyes from aqueous solution by a Zr-based metal–organic framework: Effects of Ce(III) doping, *Dalton Trans.*, 2018, vol. 47, no. 11, pp. 3913–3920.
11. Li, T.-T., Liu, Y.-M., Wang, T., Wu, Y.-L., He, Y.-L., Yang, R., and Zheng, S.-R., Regulation of the surface area and surface charge property of MOFs by multivariate strategy: Synthesis, characterization, selective dye adsorption and separation, *Microporous Mesoporous Mater.*, 2018, vol. 272, pp. 101–108.
12. Katz, M.J., Brown, Z.J., Colón, Y.J., Siu, P.W., Scheidt, K.A., Snurr, R.Q., Hupp, J.T., and Farha, O.K., A facile synthesis of UiO-66, UiO-67 and their derivatives, *Chem. Commun.*, 2017, vol. 49, no. 82, p. 9449.
13. Yang, J., Zheng, C., Xiong, P., Li, Y., and Wei, M., Zn-doped Ni-MOF material with a high supercapacitive performance, *J. Mater. Chem., A.*, 2014, vol. 2, no. 44, pp. 19005–19010.
14. Botas, J.A., Calleja, G., Sánchez-Sánchez, M., and Orcajo, M.G., Cobalt doping of the MOF-5 framework and its effect on gas-adsorption properties, *Langmuir*, 2010, vol. 26, no. 8, pp. 5300–5303.
15. Ebrahim, A.M. and Bandosz, T.J., Ce(III) doped Zr-based MOFs as excellent NO_2 adsorbents at ambient conditions, *ACS Appl. Mater. Interfaces*, 2013, vol. 5, no. 21, pp. 10565–10573.
16. Cheng, J.P., Chen, X., Wu, J.-S., Liu, F., Zhang, X.B., and Dravid, V.P., Porous cobalt oxides with tunable hierarchical morphologies for supercapacitor electrodes, *CrystEngComm.*, 2012, vol. 14, no. 20, p. 6702.
17. Mohammadi, A.A., Alinejad, A., Kamarehie, B., Javan, S., Ghaderpoury, A., Ahmadpour, M., and Ghaderpoori, M., Metal-organic framework Uio-66 for adsorption of methylene blue dye from aqueous solutions, *Int. J. Environ. Sci. Technol.*, 2017, vol. 14, no. 9, 1959–1968. .
18. Atzori, C., Shearer, G.C., Maschio, L., Civalleri, B., Bonino, F., Lamberti, C., Svelle, S., Lillerud, K.P., and Bordiga, S., Effect of benzoic acid as a modulator in the structure of UiO-66: An experimental and computational study, *J. Phys. Chem C.,* 2017, vol. 121, no. 17, pp. 9312–9324.
19. Kandiah, M., Nilsen, M.H., Usseglio, S., Jakobsen, S., Olsbye, U., Tilset, M., Larabi, C., Quadrelli, E.A., Bonino, F., and Lillerud, K.P., Synthesis and stability of tagged UiO-66 Zr-MOFs, *Chem. Mater.*, 2010, vol. 22, no. 24, pp. 6632–6640.
20. Maschio, L., Kirtman, B., Rérat, M., Orlando, R., and Dovesi, R., *Ab initio* analytical Raman intensities for periodic systems through a coupled perturbed Hartree–Fock/Kohn–Sham method in an atomic orbital basis. II. Validation and comparison with experiments, *J. Chem. Phys.*, 2013, vol. 139, no. 16, art. ID 164102.
21. Nickolov, Z., Georgiev, G., Stoilova, D., and Ivanov, I., Raman and IR study of cobalt acetate dehydrate, *J. Mol. Struct.*, 1995, vol. 354, no. 2, pp. 119–125.
22. Rivas-Murias, B. and Salgueiriño, V., Thermodynamic CoO–Co_3O_4 crossover using Raman spectroscopy in magnetic octahedron-shaped nanocrystals, *J. Raman Spectrosc.*, 2017, vol. 48, no. 6, pp. 837–841.
23. Hu, Y.H. and Zhang, L., Amorphization of metal-organic framework MOF-5 at unusually low applied pressure, *Phys. Rev. B.*, 2010, vol. 81, no. 17, p. 174103.
24. Ewen, S. and Geoffrey, D., *Modern Raman Spectroscopy: A Practical Approach*, 2nd ed., Chichester: Wiley, 2019, pp. 1–20.

25. Jiang, C., Fu, B., Cai, H., and Cai, T., Efficient adsorptive removal of Congo red from aqueous solution by synthesized zeolitic imidazolate framework-8, *Chem. Speciation Bioavailability*, 2016, vol. 28, nos. 1–4, pp. 199–208.
26. Zhang, Z.-H., Zhang, J.-L., Liu, J.-M., Xiong, Z.-H., and Chen, X., Selective and competitive adsorption of azo dyes on the metal–organic framework ZIF-67, *Water, Air Soil Pollut.*, 2016, vol. 227, no. 12.
27. Liu, X., Gong, W., Luo, J., Zou, C., Yang, Y., and Yang, S., Selective adsorption of cationic dyes from aqueous solution by polyoxometalate-based metal-organic framework composite, *Appl. Surf. Sci.*, 2016, vol. 362, pp. 517–524.
28. Hasan, Z. and Jhung, S.H., Removal of hazardous organics from water using metal-organic frameworks (MOFs): Plausible mechanisms for selective adsorptions, *J. Hazard. Mater.*, 2015, vol. 283, pp. 329–339.
29. Ayati, A., Shahrak, M.N., Tanhaei, B., and Sillanpää, M., Emerging adsorptive removal of azo dye by metal-organic frameworks, *Chemosphere*, 2016, vol. 160, pp. 30–44.
30. García, E.R., Medina, R.L., Lozano, M.M., Hernández Pérez, I., Valero, M.J., and Franco, A.M.M., Adsorption of azo-dye orange II from aqueous solutions using a metal-organic framework material: iron-benzenetricarboxylate, *Materials* (Basel), 2014, vol. 7, no. 12, pp. 8037–8057.